

pubs.acs.org/joc Article

# $\alpha$ -Cleavage of 2,2-Diazido-2,3-dihydroinden-1-one in Solution and Cryogenic Matrices

Brandi James, H. Dushanee M. Sriyarathne, Upasana Banerjee, Wandana K. S. Henarath Mohottige, Ben Crabtree, Aliz León, Miao Hong, Javeria Tariq, Taha Alhayani, Manabu Abe, Bruce S. Ault, and Anna D. Gudmundsdottir\*



Cite This: https://doi.org/10.1021/acs.joc.4c00499



ACCESS

III Metrics & More

Article Recommendations

Supporting Information

**ABSTRACT:** The Norrish type I (α-cleavage) reaction is an excellent photochemical method for radical-pair formation in solution. However, in cryogenic matrices, the starting material typically re-forms before the radical pair diffuses apart. This study focused on N<sub>2</sub> extrusion from an azido alkyl radical to prevent radical-pair recombination. Irradiation of 2,2-diazido-2,3-dihydroinden-1-one (1) in methanol mainly yielded methyl 2-cyanomethylbenzoate (2) and 2-cyanomethylbenzoic acid (3) via α-cleavage. Laser flash photolysis of 1 in argon-saturated acetonitrile resulted in α-cleavage to form triplet biradical <sup>3</sup>1Br1 ( $\lambda_{\rm max} \sim 410$  nm,  $\tau \sim 400$  ns). In contrast, upon irradiation in glassy 2-methyltetrahydrofuran matrices, triplet alkylnitrene <sup>3</sup>1N was

 $N_3$   $\alpha$ -cleavage  $N_3$   $N_3$   $N_3$   $N_4$   $N_5$   $N_5$ 

directly detected using electron spin resonance ( $D/hc = 1.5646 \text{ cm}^{-1}$ ,  $E/hc = 0.00161 \text{ cm}^{-1}$ ) and absorption spectroscopy ( $\lambda_{\text{max}} = 276 \text{ and } 341 \text{ nm}$ ). Irradiation of 1 in argon matrices generated  $^31\text{N}$ , benzoyl azide 4, singlet benzoylnitrene  $^14\text{N}$ , and isocyanide 5, as revealed by IR spectroscopy. The experimental results supported by density functional theory calculations [B3PW91/6-311++G(d,p)] suggest that irradiation of 1 in matrices results in  $\alpha$ -cleavage to form biradical  $^31\text{Br1}$ , which extrudes  $N_2$  to yield  $^31\text{Br2}$ . Rearrangement of  $^31\text{Br2}$  into  $^31\text{N}$  competes with cleavage of a  $N_3$  radical to form radical  $^12\text{Ra3}$ . The  $N_3/12\text{Ra3}$  radical pair combines to form 4, which upon irradiation yields  $^14\text{N}$  and 5.

#### ■ INTRODUCTION

One of the most studied photoreactions is the Norrish type I ( $\alpha$ -cleavage) reaction of ketones and aldehydes, in which a C-C bond adjacent to a carbonyl group cleaves to form a radical pair. As a convenient approach for producing radical pairs by simply exposing the reagents to light, this reaction has numerous applications, including the photoinitiation of polymerization and cross-linking of polymers. <sup>2ab-c</sup> In confined media, such as cryogenic matrices or crystals,  $\alpha$ -cleavage to form a radical pair has limited utility because the initial radical pair generally cannot diffuse apart and thus recombines to regenerate the starting material. <sup>3a,b</sup> However, the  $\alpha$ -cleavage of aliphatic ketones can become nonreversible if the cleavage of a second C-C bond, resulting in extrusion of a CO molecule, is faster than recombination of the initial radical pair. 4a,b Garcia-Garibay and colleagues have successfully utilized this approach to create radical pairs in crystals, which can be used for the stereoselective formation of C-C bonds in solid-state reactions. 5a,b

As another strategy for preventing a radical pair from regenerating the starting material, an azido group introduced next to a carbon-centered radical can effectively extrude a nitrogen molecule, resulting in irreversible formation of an imine radical.6 We demonstrated the use of this method in crystals to form radical pairs that yield photoproducts rather than re-form the starting material (Scheme 1). Specifically, irradiating  $\alpha$ -azido-acetophenone derivatives in the solid state yields N-methylenebenzamide derivatives. Laser flash photolysis of nanocrystals showed that the photoreaction occurs through  $\alpha$ -cleavage to form a benzoyl and methyl azido radical pair. The azido methyl radical is assumed to extrude a N<sub>2</sub> molecule, generating an imine radical that intersystem-crosses and forms a bond with the benzoyl radical. Interestingly, upon irradiation in argon matrices,  $\alpha$ -azido-acetophenone does not undergo  $\alpha$ -cleavage, instead forms the corresponding triplet alkylnitrene (Scheme 1)<sup>8</sup> through intramolecular sensitization from the triplet ketone to the azido chromophore, which extrudes a N<sub>2</sub> molecule. Presumably, intramolecular energy transfer in argon matrices is more efficient than  $\alpha$ -cleavage. In

Received: February 24, 2024 Revised: April 19, 2024 Accepted: April 25, 2024



Scheme 1. Photolysis of Azido-Acetophenone Derivatives in Crystals and Argon Matrices<sup>7,8</sup>

Ar: Ph, p-Cl-Ph, p-BrPh, 
$$N_3$$
  $N_3$   $N_3$   $N_4$   $N_4$   $N_5$   $N_5$   $N_5$   $N_6$   $N_6$   $N_8$   $N_8$ 

Scheme 2. Photolysis of 2-Azido-2-phenyl-1H-indene-1,3(2H)-dione in Argon Matrices<sup>9</sup>

contrast, laser flash photolysis of  $\alpha$ -azido-acetophenone in solution revealed that both intramolecular energy transfer and  $\alpha$ -cleavage occur to form a triplet alkylnitrene and benzoyl radical.<sup>8</sup>

Nonetheless, we found that  $\alpha$ -cleavage can result in effective product formation in argon matrices. Irradiation of 2-azido-2-phenyl-1H-indene-1,3(2H)-dione results in  $\alpha$ -cleavage to yield a biradical that extrudes a N<sub>2</sub> molecule to form an imine biradical. Subsequent rearrangement into the corresponding triplet alkylnitrene competes with intersystem crossing to form benzonitrile, benzocyclobutene-1,2-dione, and 2-aza-3-phenyl-1,4-naphthoquinone (Scheme 2).

Photoreactivity in argon matrices is generally followed using IR spectroscopy, whereas solid-state reaction mechanisms are typically elucidated using laser flash photolysis of nanosuspensions or diffuse reflectance laser flash photolysis of solids. However, as not all radicals absorb strongly, laser flash photolysis detection can be difficult. Because radical pairs can be confined within both cryogenic matrices and crystals, cryogenic matrices have the potential to facilitate or support the elucidation of solid-state photoreactions involving radical-pair formation, where one or both of the radicals does not absorb strongly.

In this study, we investigated the photoreactivity of 2,2-diazido-2,3-dihydroinden-1-one (1) in solution and cryogenic matrices to determine the influence of two azido groups attached to the  $\alpha$ -carbon atom on  $\alpha$ -cleavage. In solution, product studies and laser flash photolysis were used to investigate the photoreactivity of 1, whereas electron spin resonance (ESR), absorption, and IR spectroscopies were used in cryogenic matrices. Furthermore, density functional theory (DFT) calculations were performed to support the reaction mechanism proposed based on the experimental findings.

### ■ RESULTS AND DISCUSSION

**Product Studies.** Irradiation ( $h\nu > 300$  nm) of azide 1 in argon- and oxygen-saturated methanol at room temperature led to a complex mixture of products, as shown by GC-MS analysis of the reaction mixture. Two major products, methyl 2-cyanomethylbenzoate (2) and 2-cyanomethylbenzoic acid (3), were identified by injection of authentic samples (Scheme 3). These products formed in a ratio of 4:1 in argon-saturated

Scheme 3. Major Photoproducts Formed by Irradiating 1 in Argon- and Oxygen-Saturated Methanol

methanol and 1:1.5 in oxygen-saturated methanol, with 2 being the major photoproduct in argon-saturated methanol and 3 in oxygen-saturated methanol. Similarly, preparative photolysis of 1 in argon-saturated dry methanol resulted in formation of 2 as the major product and a lesser amount of 3. However, it should be noted that the reaction resulted in a significant amount of polymeric tar formation.

The formation of products 2 and 3 demonstrates that 1 undergoes  $\alpha$ -cleavage, which is theorized to occur as shown in Scheme 4. The triplet configuration of the ketone  $(T_K)$  in 1 cleaves to form biradical  ${}^31Br1$ , which extrudes a  $N_2$  molecule to yield imine biradical  ${}^31Br2$ . Biradical  ${}^31Br2$  can expel a  $N_3$  radical to form radical  ${}^11Ra3$ . The  $N_3$  radical can abstract a H atom from  ${}^111Ra3$  to form ketene  ${}^111Ra3$ , which is trapped by methanol or moisture to form products 2 and 3, respectively. It is also possible that in oxygen-saturated solution, 3 is formed by oxygen trapping of  ${}^111Ra3$ , as benzoyl radicals react efficiently

Scheme 4. Proposed Mechanism for Forming Products 2 and 3 upon Irradiating 1 in Methanol

with oxygen. <sup>11a,b</sup> However, we cannot rule out  $T_{\rm K}$  of 1 decaying by energy transfer to form the triplet excited state of the azido chromophore ( $T_{\rm A}$ ) of 1 with subsequent extrusion of a  $N_2$  molecule to form <sup>3</sup>1N, which undergoes  $\alpha$ -cleavage to yield <sup>3</sup>1Br2.

**ESR Spectroscopy.** To determine whether irradiation of 1 yields nitrene  $^3$ 1N, a nitrogen-saturated 2-methyltetrahydrofuran (mTHF) solution of 1 was cooled to 80 K and irradiated while recording ESR spectra between 0 and 10,000 G. The spectra showed  $X_2$  and  $Y_2$  lines typical of an alkyl nitrene at 8163 and 8254 G, respectively (Figure 1). Zero-field splitting (ZFP) parameters of D/hc = 1.5646 cm<sup>-1</sup> and E/hc = 0.00161

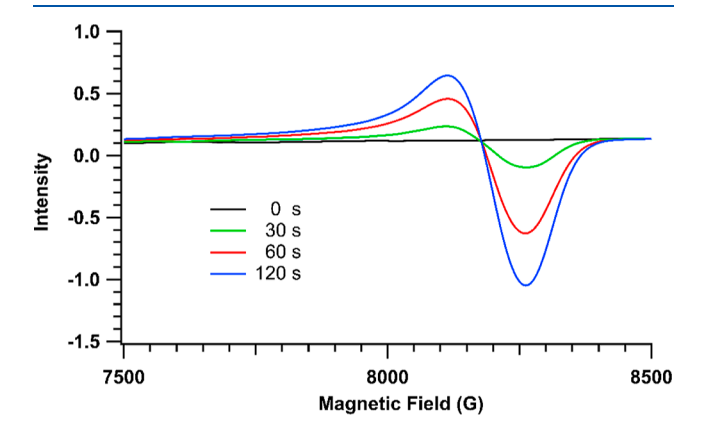


Figure 1. ESR spectra of  ${}^31N$  as a function of irradiation time of 1 in mTHF matrices. Full spectra between 0 and 10,000 G is presented in the Supporting Information (Figure S1) and the ESR signal at ~8500 G is a function of irradiation of 1 up to 25 min.

cm<sup>-1</sup> were calculated based on the  $X_2$  and  $Y_2$  lines using Wasserman's equations. <sup>12a,b</sup> As the ZFP parameters of 1 are similar to previously reported ESR data for triplet alkylnitrenes, we assigned the observed signals to <sup>3</sup>1N. <sup>9,13</sup> Although ESR spectroscopy confirmed the formation of <sup>3</sup>1N, we could not determine whether it originated from  $T_K$  of 1 undergoing energy transfer to the azido chromophore or  $\alpha$ -cleavage (Scheme 2).

Absorption Spectroscopy in Glassy mTHF Matrices. Because ESR spectroscopy verified the formation of <sup>3</sup>1N in a glassy matrix, we investigated the absorption spectrum of this species using similar experimental conditions. Irradiation of 1 in a glassy mTHF matrix resulted in new broad absorption bands at 240–250 nm ( $\lambda_{\rm max}$  ~ 241 nm), 270–300 nm ( $\lambda_{\rm max}$  ~ 276 nm), and 313–350 nm ( $\lambda_{\rm max}\sim$  320 nm) with a small shoulder at ~335 nm (Figure 2A). With further irradiation of the matrix, these bands increased in intensity, whereas the bands at 258, 265, and 307 nm, which correspond to the ground-state absorption of 1 (Figures S2 and S3), decreased. The newly formed experimental bands agreed well with the major time-dependent DFT (TD-DFT)-calculated electronic transitions of  ${}^{3}$ **IN** (Figure 2B) at 240 nm (f = 0.077), 252 nm (f = 0.019), 265 nm (f = 0.022), 305 nm (f = 0.014), 314 nm (f = 0.026), and 356 nm (f = 0.0083). Thus, the new absorption bands were assigned to <sup>3</sup>1N.

**Laser Flash Photolysis.** The excited states and reactive intermediates formed in solution upon irradiating 1 were investigated using laser flash photolysis. Laser flash photolysis ( $\lambda = 266$  nm) of 1 in argon-saturated methanol produced transient absorption with a broad band at 300–550 nm ( $\lambda_{\text{max}} = \sim 320$  and 410 nm) (Figure 3). Similar transient absorption

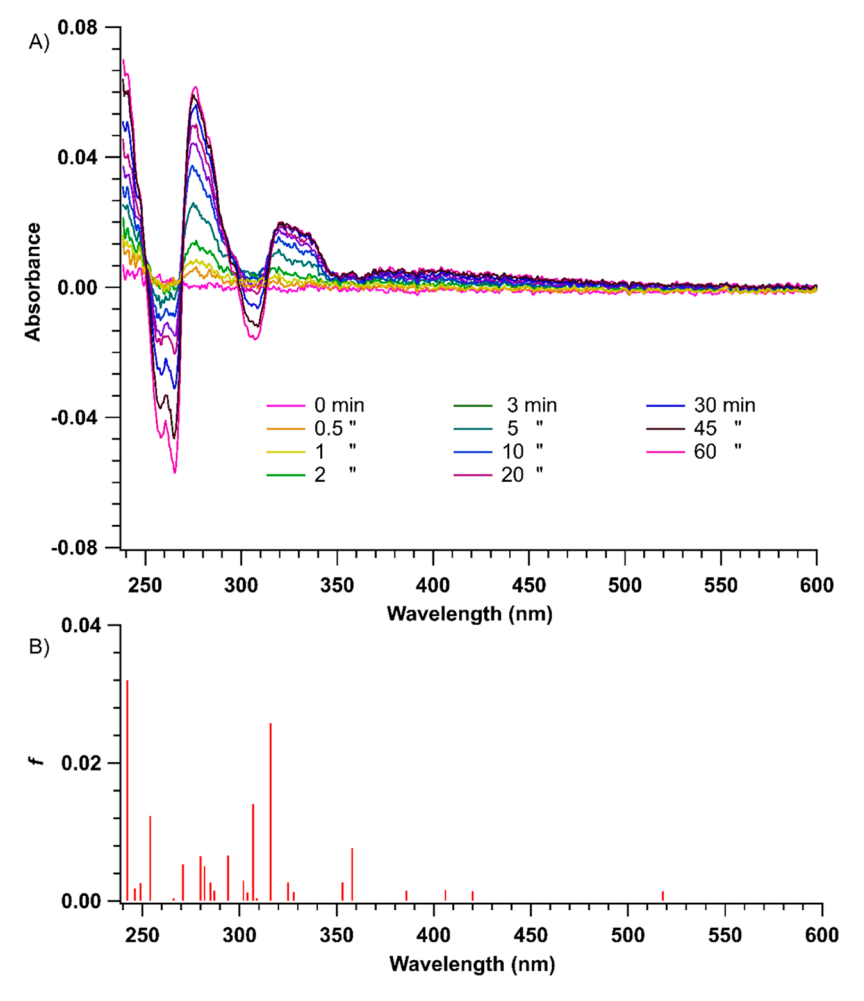
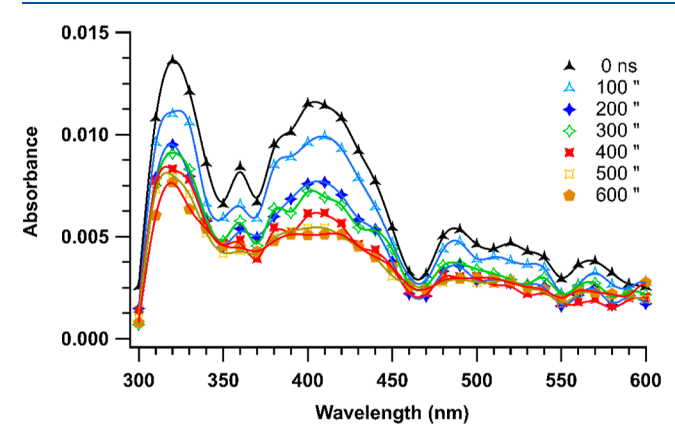


Figure 2. (A) Absorption difference spectra obtained by subtracting the initial spectrum of 1 from the spectra collected during irradiation of 1 at 77 K. (B) TD-DFT-calculated spectrum of  $^31N$  at the B3PW91/6-311++G(d,p) level of theory.



**Figure 3.** Transient absorption spectra obtained by laser flash photolysis of **1** in argon-saturated acetonitrile.

spectra were observed when laser flash photolysis was performed using a 308 nm laser (Figure S3); thus, the photochemistry of 1 is not wavelength-dependent.

The transient absorption exhibited the same kinetic profile across the transient absorption spectrum (Figures 4 and S5–S8). In argon-saturated acetonitrile, the decay was best fitted as a monoexponential function with residual absorption that did not decay on a microsecond time scale. Fitting of the short-lived component yielded a lifetime of 402 ns ( $k = 2.49 \times 10^6$ 

s<sup>-1</sup>). The lifetime became shorter in air- and oxygen-saturated acetonitrile [380 ns ( $k = 2.63 \times 10^6 \text{ s}^{-1}$ ) and 225 ns (k = 4.44 $\times$  10<sup>6</sup> s<sup>-1</sup>), respectively]. Based on the estimated oxygen concentrations in air- and oxygen-saturated acetonitrile (1.9 and 9.1 mM, respectively), 14 the rate constant for oxygen quenching of the transient absorption is between 4.9 and 14 × 108 M<sup>-1</sup> s<sup>-1</sup>. This rate constant is close to the diffusioncontrolled limit, suggesting that the transient is not <sup>3</sup>1N, as alkylnitrenes react with oxygen with a lower rate constant. 13 In addition, triplet alkylnitrenes generally have lifetimes of several hundreds of microseconds or longer<sup>8,13</sup> and their transient spectra differ from the absorption spectrum of <sup>3</sup>1N in glassy mTHF. Based on the TD-DFT-calculated absorption spectra of T<sub>K</sub> of 1, <sup>3</sup>1Br1, and <sup>3</sup>1Br2 (Figure 5), the observed transient absorption spectrum corresponds well with the calculated spectrum of <sup>3</sup>1Br1. There is residual absorbance that can potentially be assigned to formation of <sup>3</sup>**1Br2**, however, as the residual absorbance is weak it is complicated to confirm the assignment to <sup>3</sup>1Br2. It should be noted that the calculated spectrum of 1Ra3 does not have electronic transitions above 300 nm; thus, this species cannot be observed using laser flash photolysis (Figure S9). The laser flash photolysis results indicate that 1 undergoes efficient  $\alpha$ -cleavage in solution and that the lifetime of T<sub>K</sub> of 1 is less than the time resolution of the laser flash photolysis system (2-3 ns).

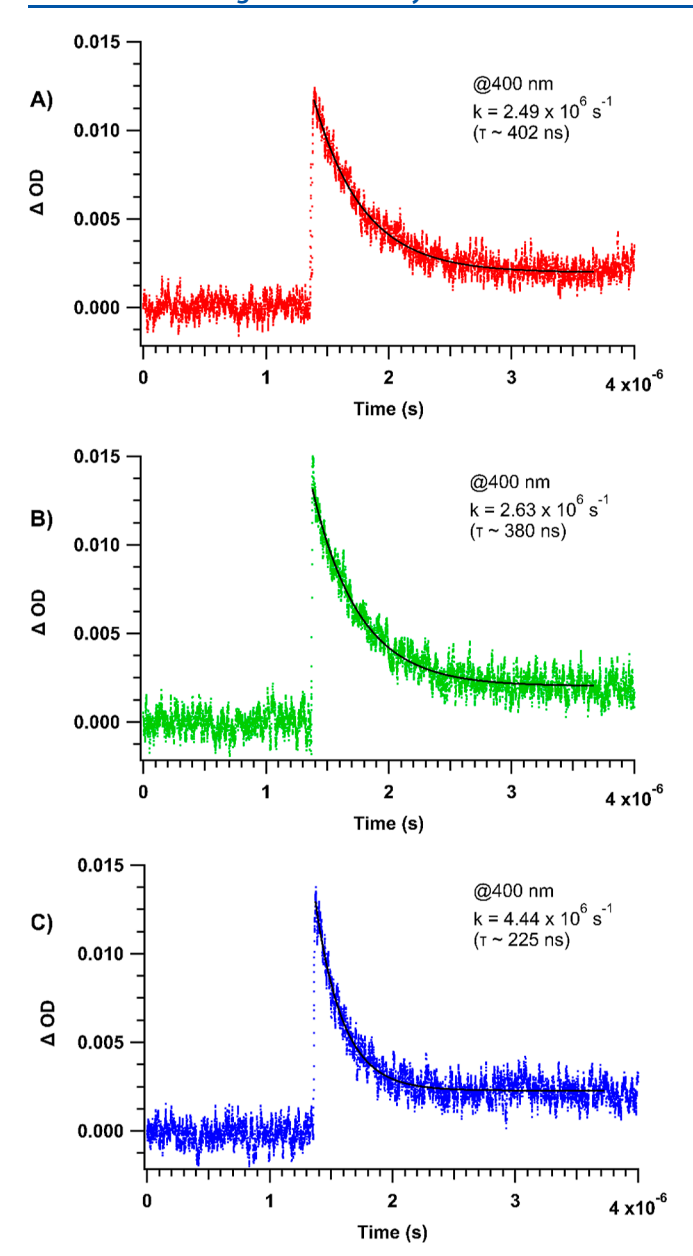


Figure 4. Kinetic traces at 400 nm obtained by laser flash photolysis of 1 in (A) argon-, (B) air-, and (C) oxygen-saturated acetonitrile.

**Phosphorescence.** Because we did not observe  $T_K$  of 1 using laser flash photolysis, the formation of this species upon irradiating 1 was confirmed using phosphorescence measurements at 77 K in ethanol (Figure 6). The emission onset was estimated to be 418 nm, which corresponds to  $T_K$  of 1 having an energy of 68 kcal/mol.

**Matrix Isolation.** Azide 1 undergoes α-cleavage in solution, whereas  $^3$ 1N is observed in glassy matrices. To determine the pathway for forming  $^3$ 1N and verify whether 1 undergoes α-cleavage in matrices, we followed the photoreactivity of 1 in an argon matrix at 6 K using IR spectroscopy (Figures 7 and 8). The IR spectrum of 1 showed intense azido bands at 2157, 2127, 2109, and 2082 cm<sup>-1</sup> with additional major bands at 1734, 1615, 1246, 1218, 1210, 1018, 911, and 710 cm<sup>-1</sup>. The various azido bands are presumably due to different conformers of 1 being entrapped in different matrix sites. Irradiation led to depletion of the bands corresponding to 1 and the formation of new bands at 2288, 2266, 2140, 2090,

1769, 1723, 1710, 1593, 1526, 986, 936, 758, and 742 cm<sup>-1</sup> (Figures 7 and 8A). Because ESR spectroscopy verified the formation of <sup>3</sup>1N, we assigned the bands at 2090, 1723, 1593, and 936 cm<sup>-1</sup> to this species, as these bands fit with the calculated and scaled bands (see Quantum Chemical Calculations for details) of <sup>3</sup>1N at 2191, 1756, 1598, and 934 cm<sup>-1</sup> (Figure 8B). The intensity of these bands increased throughout irradiation. In contrast, the intensity of the bands formed at 2140, 1710, and 986 cm<sup>-1</sup> increased for the first  $\sim$ 40 min and then decreased. We assigned these bands to 2cyanomethyl benzoyl azide (4) by comparison with its calculated spectrum, which has major bands at 2224, 1684, 1257, and 976 cm<sup>-1</sup> (Figure 8B). This assignment was further supported by comparison of the IR spectrum of 4 with that reported for its derivative, benzoyl azide (PhCON<sub>3</sub>), in argon matrices, which exhibits a strong azido band at 2140 cm<sup>-1</sup> and carbonyl stretch at 1692 cm<sup>-1</sup> 15a,b Similarly, the bands at 2288, 2266, 1526, and 742 cm<sup>-1</sup> were assigned to 2cyanomethylphenyl isocyanate (5) because they correspond well with the most intense bands in its calculated spectrum at 2290, 1506, and 742 cm<sup>-1</sup> (Figure 8B). This assignment was supported by comparison with the IR spectrum of phenyl isocyanate, a derivate of 5. The N=C=O bands of phenyl isocyanate were observed at 2289 and 2266 cm<sup>-1</sup> by Toscano and co-workers, who suggested that the splitting of this signal is due to Fermi resonance, 16 as these bands appear as a doublet in chloroform solution (2278 and 2260 cm<sup>-1</sup>).<sup>17</sup> Finally, the bands at 1769 and 758 cm<sup>-1</sup> were assigned to singlet benzoylnitrene <sup>1</sup>4N, which has calculated and scaled bands at 1757 and 756 cm<sup>-1</sup> (Figure 8B). This assignment was supported by the observation of a C=O band at 1760 cm $^{-1}$ for its derivative, singlet benzoylnitrene [Ph-C(O)-N], in acetonitrile, as revealed using time-resolved IR spectroscopy. As the IR bands corresponding to <sup>1</sup>4 and 5 only began to grow after irradiating for 10 min, these species are concluded to be secondary photoproducts formed by the photolysis of 4, similar to the behavior reported for benzoyl azide. 16,18

To further support the formation of <sup>1</sup>4N and 5, we synthesized 1 using 15N-labeled sodium azide. In the obtained product (1-15N), 50% of the  $\alpha$ - and  $\gamma$ -N atoms were labeled with <sup>15</sup>N (Scheme 5). Upon irradiating 1-<sup>15</sup>N in an argon matrix, we examined the IR bands that changed upon isotope labeling by comparison with the IR spectra calculated for <sup>1</sup>4N and 5 with all possible isotope substitution patterns (Supporting Information). For <sup>1</sup>4N, the C-N stretching bands were located at 1769 and 1756 cm<sup>-1</sup> (Figure 9B), which agrees with the calculated and scaled bands at 1757 and 1742 cm<sup>-1</sup> with <sup>1</sup>4N and <sup>15</sup>N, respectively. Isotope labeling shifted the isocyanate bands of 5 to 2281, 2271, and 2264 cm (Figure 9A). As mentioned earlier, the splitting of the N=C=O band has been attributed to Fermi resonance, which presumably originates from coupling of the N=C=O band with the combination mode arising from the bands at 1526 and  $742 \text{ cm}^{-1}$  (1526 + 742 = 2268). Thus, isotope labeling changes the Fermi splitting, with the 2288 cm<sup>-1</sup> band shifting to 2281 cm<sup>-1</sup>. The calculated bands for isotope-labeled N=C=O were located at 2290, 2279, and 2278 cm<sup>-1</sup>, which matches well with the observed bands. Because the azido bands of 1, <sup>3</sup>1N, and 4 overlap, these bands could not be assigned accurately after isotope labeling.

Finally, we compared the depletion rate of the 1734 cm<sup>-1</sup> band corresponding to 1 with the formation rates of the IR bands at 2288, 1769, 1723, and 1710 cm<sup>-1</sup> corresponding to 5,

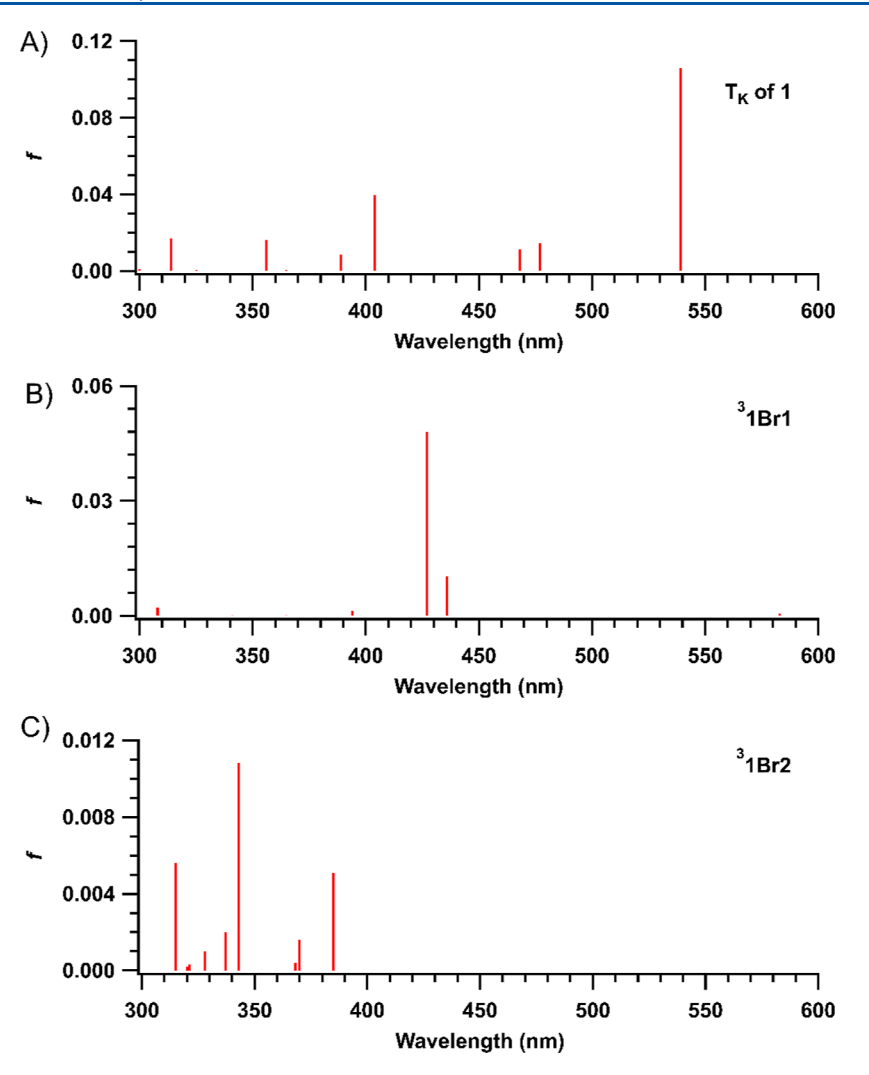


Figure 5. TD-DFT-calculated absorption spectra of (A) T<sub>K</sub> of 1, (B) <sup>3</sup>1Br1, and (C) <sup>3</sup>1Br2 at the B3PW91/6-311++G(d,p) level of theory.

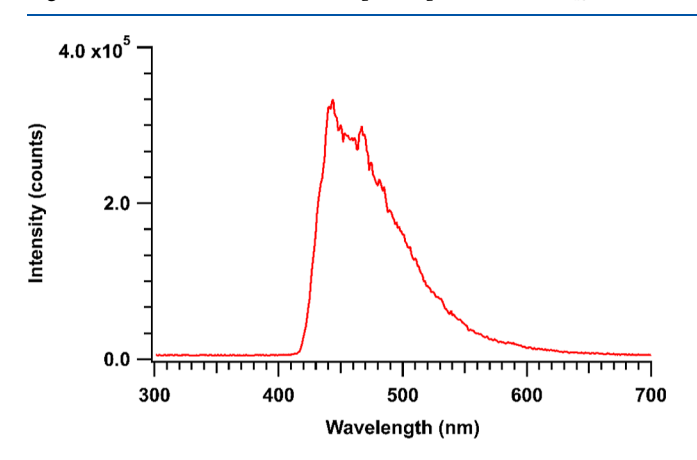


Figure 6. Phosphorescence spectrum obtained by irradiating  $1\ (266\ nm)$  in ethanol at  $77\ K$ .

<sup>1</sup>4N, <sup>3</sup>1N, and 4, respectively (Figure S10). Interestingly, during the first 60 min of irradiation, the band of 1 was depleted at the same rate as the bands of <sup>3</sup>1N and 4 were formed, within experimental error. After 60 min, the 1710 cm<sup>-1</sup> band of 4 began to decrease in intensity, whereas the band at 1723 cm<sup>-1</sup> continued to grow at a rate similar to that for the depletion of the band of 1. Thus, we concluded that <sup>3</sup>1N and 4 are formed from the same precursor, <sup>3</sup>1Br2. As the

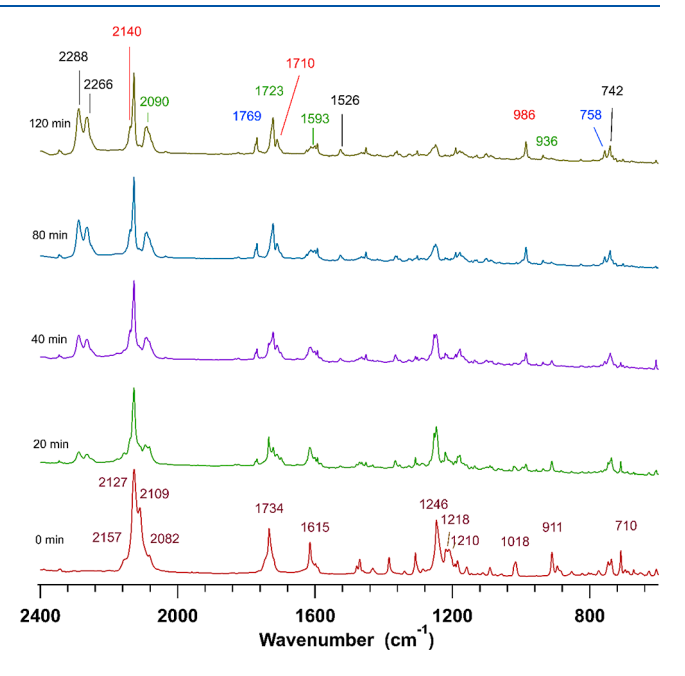


Figure 7. IR spectra obtained by irradiating  ${\bf 1}$  in an argon matrix at  ${\bf 6}$  K

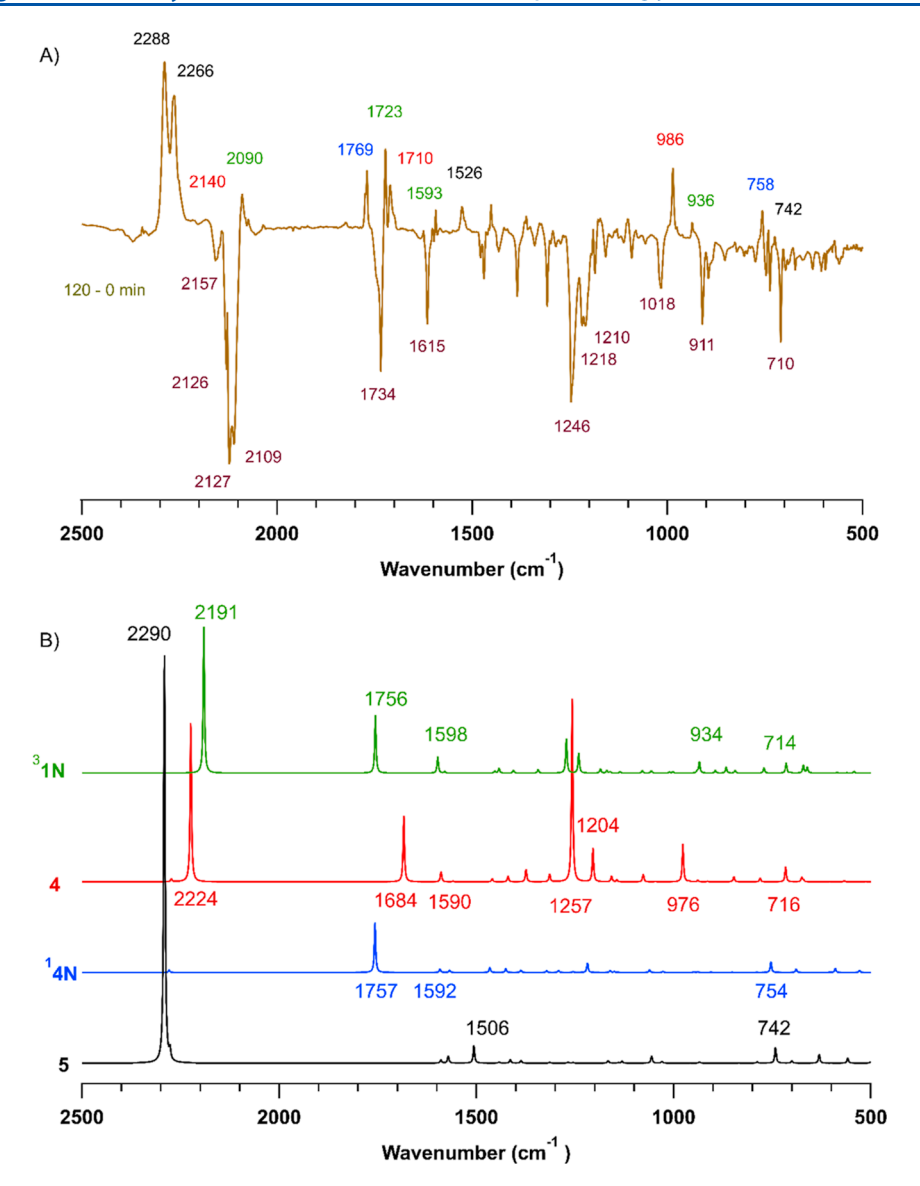


Figure 8. (A) IR difference spectrum obtained by subtracting the initial spectrum of 1 from that collected after irradiation of 1 for 120 min in an argon matrix. The negative bands correspond to 1, whereas the positive bands correspond to photoproducts  ${}^{3}$ 1N, 4,  ${}^{1}$ 4N, and 5. (B) Calculated IR spectra of  ${}^{3}$ 1N, 4,  ${}^{1}$ 4N, and 5 at the B3PW91/6-311++G(d,p) level of theory.

Scheme 5. 15N Isotope Labeling of 1 and Its Photoproducts 4, 31N, 14N, and 5

bands of  $^14N$  and 5 grew at similar rates, these species must both be formed from 4; however, we could not determine accurately whether  $^14N$  yields 5. Based on these findings, we proposed a mechanism for the photoreactivity of 1 in cryogenic matrices, as shown in Scheme 6. Specifically,  $T_K$  of 1 decays by  $\alpha$ -cleavage to form  $^31Br1$ , which extrudes a  $N_2$  molecule to form  $^31Br2$ . Interestingly,  $^31Br2$  can rearrange to form  $^31N$  or extrude a  $N_3$  radical to yield  $^14Ra3$ . Because diffusion is limited in argon matrices, the  $N_3$  and  $^14Ra3$  radical pair combine to form benzoyl azide 4. Irradiation of 4 yields

benzoylnitrene <sup>1</sup>4N and isocyanide 5. Notably, we could not unambiguously attribute any IR bands to the formation of triplet benzoylnitrene <sup>3</sup>4N, for which the major bands were calculated to appear at 1588 (76), 1475 (416), 1453 (130), and 1194 (337) cm<sup>-1</sup>. In addition, it should be noted that Jenks and co-workers reported that the time-resolved IR spectrum of *N*-benzoyl-dibenzothiophenesulfilimine exhibits a band at 1485 cm<sup>-1</sup> assigned to triplet benzoylnitrene.<sup>19</sup>

**Calculations.** To support the mechanism in Scheme 6, we calculated stationary points on the singlet and triplet surfaces

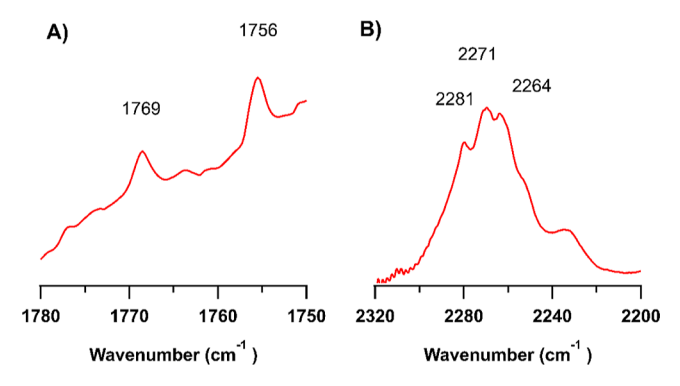


Figure 9. IR bands assigned to (A) 5 and (B) <sup>1</sup>4N upon irradiation of 1-<sup>15</sup>N in an argon matrix.

Scheme 6. Proposed Mechanism for Forming <sup>3</sup>1N, 4, <sup>1</sup>4N, and 5 upon Irradiating 1 in Matrices

of 1 using Gaussian16 at the B3PW91 level of theory with the 6-311++G(d,p) basis set. <sup>20abc-d</sup> Optimization of 1 resulted in two minimal energy conformers, 1A and 1B, which have the azido group at different orientations (Figures 10 and 11 and Supporting Information). TD-DFT calculations located the first singlet excited state (S<sub>1</sub>) and T<sub>K</sub> of 1 at 77 and 68 kcal/ mol, respectively, above the ground state  $(S_0)$  of 1. The optimized structure of T<sub>K</sub> of 1 was located ~66 kcal/mol above S<sub>0</sub> of 1, which is similar to the energies determined via phosphorescence measurements and TD-DFT calculations. Spin density calculations showed that the unpaired electrons are mainly located on the O and C atoms of the carbonyl group with a smaller spin density on the phenyl ring, indicating that  $T_K$  of 1 has a  $\pi$ , $\pi^*$  configuration. This result is consistent with the lack of strong vibrational bands in the phosphorescence spectrum of 1. The optimized structure of TA of 1 was located 47 kcal/mol above the So of 1 and had a N-N-N bond angle of  $\sim 120^{\circ}$ , which is typical for triplet azido groups.

The optimized structures of nitrene  $^31N$  and a  $N_2$  molecule were 19 kcal/mol more stable than  $S_0$  of 1. For  $^31N$ , the spin density calculations indicated that the unpaired electrons are mainly located on the N atom (1.84), as expected for a triplet alkylnitrene. Biradical  $^31Br1$  was located 59 kcal/mol above the  $S_0$  of 1, and spin density calculations placed the unpaired electrons mainly on the carbonyl C atom and the C atom attached to the azido groups. In comparison,  $^31Br2$  and a  $N_2$  molecule were 12 kcal/mol more stable than  $S_0$  of 1 with the unpaired electrons located on the imine N atom and the carbon atom of the carbonyl group. Optimization revealed that 1Ra3 is 7 kcal/mol more stable than  $S_0$  of 1. Finally, we optimized 1K which is 35 kcal/mol more stable than  $S_0$  of 1.

As the calculated transition-state barrier for T<sub>K</sub> of 1 undergoing  $\alpha$ -cleavage was small ( $\sim$ 2 kcal/mol), this reaction is feasible. Similarly, the calculated transition-state barrier for <sup>3</sup>1Br1 cleaving to form <sup>3</sup>1Br2 was only 3 kcal/mol. The calculated transition-state barrier for <sup>3</sup>1Br2 cleaving to form 1Ra3 and a N<sub>3</sub> radical was considerably larger (18 kcal/mol). Importantly, a similar transition-state barrier of 18 kcal/mol was calculated for <sup>3</sup>1Br2 rearranging into <sup>3</sup>1N. Thus, it is feasible that <sup>3</sup>1Br2 forms either <sup>3</sup>1N or 1Ra3. The calculated transition-state barrier for N<sub>3</sub> radical abstracting a H atom from 1Ra3 is only 9 kcal/mol. We compared the calculated stationary points on the energy surface of 1 for obtaining nitrene <sup>3</sup>1N via rearrangement of <sup>3</sup>1Br2 (Figure 12) and via energy transfer from  $T_K$  of 1 to form  $T_A$  of 1. Interestingly, the calculated transition-state barrier for <sup>3</sup>1N forming <sup>3</sup>1Br2 was 25 kcal/mol. Consequently, this transformation is unlikely to occur, consistent with <sup>3</sup>1N not being detected using laser flash photolysis.

We also optimized the structures of benzoyl azide 4 and its photoproducts <sup>1</sup>4N and 5 (Figure 13). Photoproducts <sup>1</sup>4N and 5 were located 5 and 85 kcal/mol, respectively, below the S<sub>0</sub> of 4. It should be noted that the broken symmetry method was used to optimize the structure of <sup>1</sup>4N.<sup>21a,b</sup> In addition, we optimized the structure of <sup>3</sup>4N, which was 2 kcal/mol more stable than <sup>1</sup>4N. However, this energy gap between the singlet and triplet configurations is within the calculation error. Thus, these results are similar to the findings of Toscano and coworkers for benzoylnitrene, where the triplet and singlet configurations of benzoylnitrene optimized using B3LYP/6-31G\* suggest that the triplet is more stable, <sup>16</sup> whereas more accurate methods, such as CCSD(T)/aug-cc-pVTZ//B3LYP/6-311++G(3df,3pd), indicate that singlet benzoylnitrene is the ground state.<sup>22</sup>

The stationary points for benzoyl azide 4 forming  $^14N$  and 5 were calculated (Figure 14), although we did not attempt to calculate the transition-state barriers on the singlet excited surface. TD-DFT calculations located the  $S_1$  of 4 at 75 kcal/mol above the  $S_0$  of 4. In contrast, the optimized structure of  $T_1$  of 4 was located 58 kcal/mol above the  $S_0$  of 4, and the calculated transition-state barrier for  $T_1$  of 4 extruding a  $N_2$  molecule to form  $^34N$  was only  $\sim 1$  kcal/mol. Thus, these calculations indicate that  $S_1$  of 4 does not intersystem-cross to its triplet configuration because the singlet—triplet energy gap is significant (17 kcal/mol). This behavior is consistent with the results of Platz and co-workers, who demonstrated that laser flash photolysis of benzoyl azide in solution yields singlet benzoylnitrene.  $^{15a}$ 

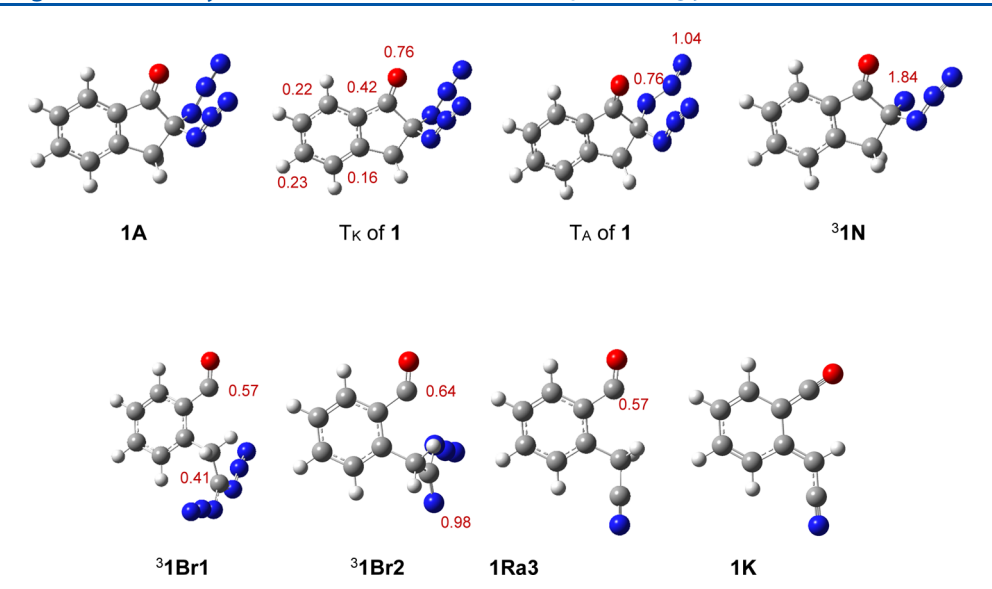


Figure 10. Optimized structures of 1A,  $T_K$  of 1,  $T_A$  of 1, T

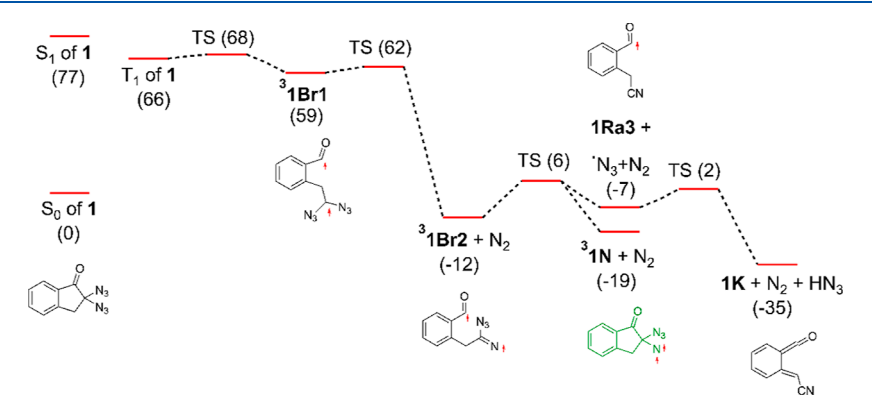


Figure 11. Calculated [B3PW91/6-311++G(d,p)] stationary points on the energy surface of 1 to yield  $^31N$  via rearrangement of  $^31Br2$ . Energies are in kcal/mol.

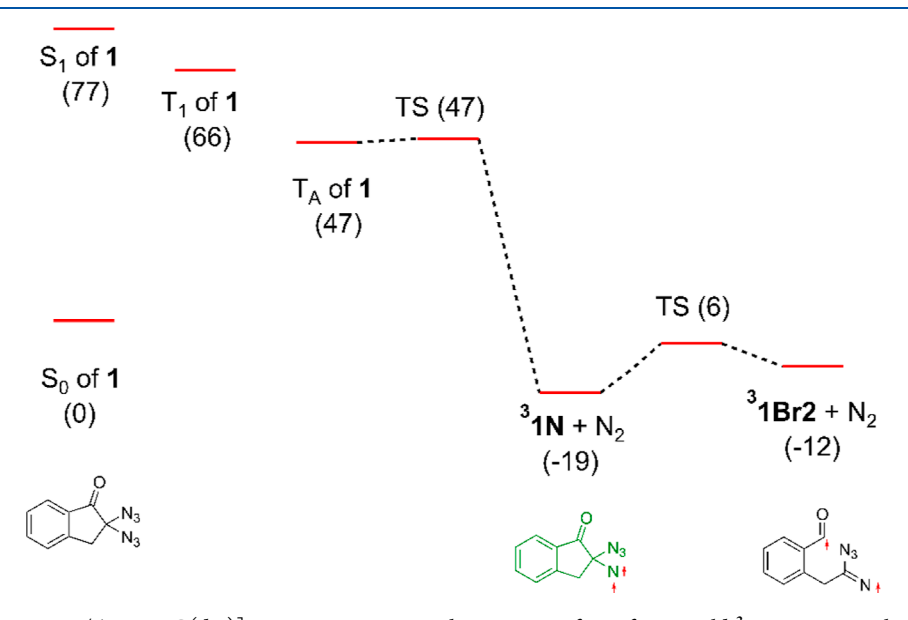


Figure 12. Calculated [B3PW91/6-311++G(d,p)] stationary points on the energy surface of 1 to yield  ${}^31N$  via intramolecular triplet sensitization from  $T_K$  of 1 to form  $T_A$  of 1. Energies are in kcal/mol.

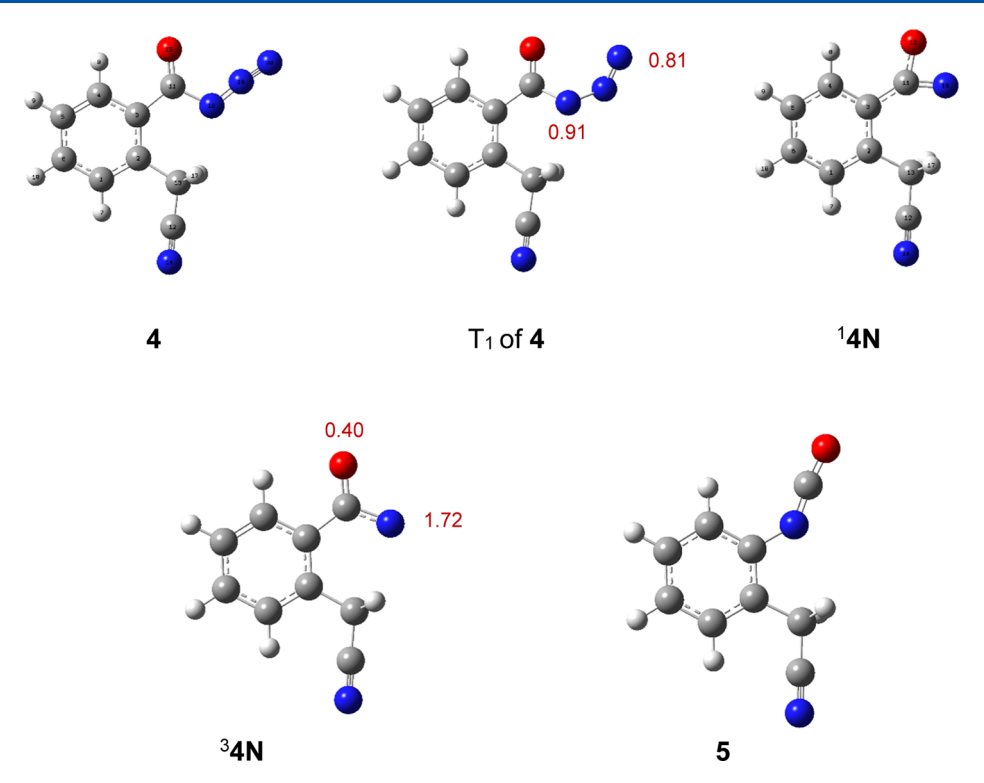


Figure 13. Optimized structures of 4,  $T_1$  of 4,  $^14N$ ,  $^34N$ , and 5 at the B3PW91/6-311++G(d,p) level of theory. The calculated spin densities are shown in red.

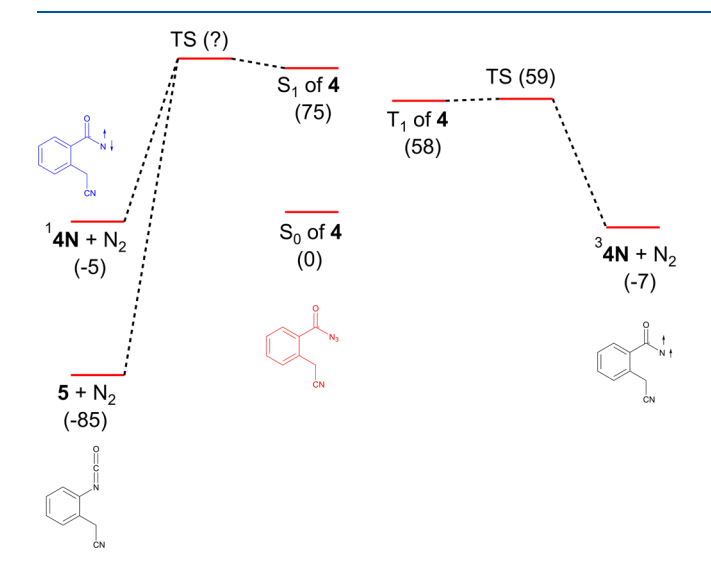


Figure 14. Calculated [B3PW91/6-311++G(d,p)] stationary points on the energy surface of 4 to yield  $^14N$ ,  $^34N$ , and 5. Energies are in kcal/mol.

# CONCLUSIONS

We demonstrated that 1 undergoes efficient  $\alpha$ -cleavage in solution to form  ${}^31\mathrm{Br1}$ , which yields products 2 and 3. Because  $\mathrm{N}_2$  extrusion from  ${}^31\mathrm{Br1}$  to yield  ${}^31\mathrm{Br2}$  is efficient enough to compete with recombination, this reaction also occurs in argon matrices. Furthermore, the presence of two azido moieties on the  $\alpha$ -carbon atom allows  ${}^31\mathrm{Br2}$  to undergo further cleavage in argon matrices to form a  $\mathrm{N}_3$  and  $1\mathrm{Ra3}$  radical pair, which combines to yield 4. In addition,  ${}^31\mathrm{Br2}$  can rearrange to  ${}^31\mathrm{N}$ . Although we cannot rule out that some  ${}^31\mathrm{N}$  is formed via intramolecular sensitization, the formation of this species in solution was not observed using laser flash photolysis. The

photoreactivity of 4 in argon matrices is similar to that observed for its derivative, benzoyl azide. These results highlight that  $\alpha$ -cleavage of 1 is feasible in argon matrices and that the second azido moiety in 1 leads to unique photoreactivity in argon matrices. Further investigation is required to determine whether crystalline derivatives of 1 exhibit the same photoreactivity and the generality of using photoreactivity in cryogenic matrices to aid with elucidating the mechanisms of solid-state photoreactions.

## EXPERIMENTAL SECTION

**ESR Spectroscopy.** An anhydrous mTHF solution of 1 (4 mg in 0.1 mL) was transferred into an ESR tube, which was then capped with a rubber septum. After degassing the solution by bubbling with nitrogen for 10 min, the tube was sealed with parafilm and placed in the ESR spectrometer (Bruker X-band EPR ES00 spectrometer). The sample was irradiated for 20 min using a Hg lamp (model L9566-01, LIGHTNINGCURE Spot Light Source LC8, Hamamatsu) with a 300–400 nm filter placed adjacent to the ESR cavity, and then the continuous-wave X-band ESR spectrum was recorded.

IR Spectroscopy in Argon Matrices. Matrix isolation was performed using two different setups. For unlabeled 1, argon was deposited at 20 K for 5 min on a cesium iodide (CsI) window inside the cryostat cold head. Subsequently, 1 was sublimated at 323 K (50 °C) and deposited along with argon for 120 min on the CsI window at 20 K. The cryostat was cooled to 9 K before irradiating the sample. The argon matrix containing 1 was irradiated through a quartz window using a Xe lamp (model SM0101, JASCO) with a 300-400 nm filter placed adjacent to the quartz window, and IR spectra were recorded after various irradiation times. For 1-15N, the matrix isolation studies were performed using conventional equipment, which has been described previously.<sup>23</sup> After depositing argon at 22 K on a CsI window, argon and the sample were deposited at room temperature for 46 min under vacuum. The system was cooled to 12 K before irradiating the sample through a quartz window using a 254 nm UV pen, and IR spectra were recorded at various irradiation times.

Laser Flash Photolysis. Laser flash photolysis was performed using a commercially available laser flash photolysis system (LP980, Edinburgh Instruments, Inc.) with laser irradiation at 266 nm (Nd:YAG, Surelite II, Continuum, Inc.) or 308 nm (excimer laser). 6,24 All spectra and kinetic traces were obtained at room temperature in a flow cell with a path length of 1 cm at a flow rate of 1 mL/min. A stock solution was prepared using spectroscopic-grade methanol or acetonitrile. The absorption of each sample was between 0.2 and 0.8 at 266 or 308 nm.

Absorption Spectroscopy in Glassy mTHF Matrices. UV—vis spectroscopy in glassy matrices was performed using a conventional setup. <sup>25</sup> A stock solution of 1 in anhydrous mTHF (0.2 mM) was prepared, which had an absorbance of less than 1 at  $\lambda_{\rm max}$  (260 nm). The solution (2 mL) was placed in a temperature-resistant 10 mm × 10 mm quartz cuvette. After purging with argon gas for 2 min, the cuvette was sealed. The cuvette was inserted in a cryostat and the UV—vis spectrum of 1 in mTHF was recorded as the baseline. Liquid nitrogen was poured into the cryostat until the temperature reached 77 K and a glassy mTHF matrix of 1 was obtained. The matrix was irradiated using a 254 nm UV pen, and difference spectra were recorded at various irradiation times.

**Phosphorescence.** A 5 mM ethanol solution of **1** was prepared, and the phosphorescence spectrum was recorded (Horiba Instruments) at 77 K using a previously described setup.  $^{26}$  The sample was irradiated at 266 nm and the emission spectrum was recorded between 300 and 800 nm.

**Quantum Chemical Calculations.** All geometries were optimized at the B3PW91 level of theory with the 6-311++G(d,p) basis set, as implemented in the Gaussian16 program at the Ohio Supercomputer Center.  $^{20\text{abc}-d}$  The absorption spectra were calculated using TD-DFT.  $^{27\text{a,b}}$  The calculated IR spectra of the intermediates and products were obtained using frequency calculations at the B3PW91 level of theory with the 6-311++G(d,p) basis set, and IR bands were scaled 0.961. The transition states were confirmed to have one imaginary vibrational frequency by analytical determination of the second derivative of the energy with respect to the internal coordinates. Intrinsic reaction coordinate calculations were used to verify that each transition state was correlated with its products and precursors.  $^{29}$ 

**Synthesis of Starting Materials.** *Synthesis of 2,2-Dibromo-2,3-dihydroinden-1-one.* 2,2-Dibromo-2,3-dihydroinden-1-one was prepared as previously reported. To a solution of 1-indanone (5.00 g, 37.8 mmol) in acetic acid (50 mL), bromine (13.3 g, 100 mmol) was added and the solution was refluxed for 1 h. After cooling to room temperature, the solution was poured onto crushed ice (100 g). The obtained solid was filtered, washed with cold water, and dried to give the desired product (8.70 g, 30 mmol, 30% yield). mp 123–126 °C (lit. mp 131–133.8 °C). IR (solid): 3060, 1715, 1603 cm<sup>-1</sup>. HNMR (CDCl<sub>3</sub>, 400 MHz): δ 7.95 (d, 1H, J = 8 Hz), 7.74 (t, 1H, J = 7.6 Hz), 7.50 (t, 1H, J = 7.6 Hz), 7.41 (d, 1H, J = 8 Hz), 4.29 (s, 2H).  $^{13}$ C{1H} NMR (CDCl<sub>3</sub>, 101 MHz): δ 192.7, 147.1, 137.0, 129.1, 129.0, 126.6, 126.1, 57.0, 52.4. GC–MS/MS (m/z): 287.9/289.9/291.9 ( $M^+$ ).

Synthesis of 2,2-Diazido-2,3-dihydroinden-1-one (1). To 2,2dibromo-2,3-dihydroinden-1-one (100 mg, 0.349 mmol), 10 mL of acetone was added. Then, sodium azide (100 mg, 4.41 mmol) dissolved in 5 mL of water was added. After stirring the resulting mixture at room temperature for 24 h, the solvent was removed under vacuum. The reaction mixture was extracted with diethyl ether (30 mL), and the organic layer was washed with water, dried with magnesium sulfate, and concentrated under vacuum. The crude product was purified via extraction using a 95:5 hexane/diethyl ether mixture to yield 1 as a yellow oil (309 mg, 1.44 mmol, 83% yield). The IR and <sup>1</sup>H NMR spectra of 1 matched those in the literature. IR (neat)  $\delta$ : 3077, 2928, 2098, 1722, 1609 cm<sup>-1</sup>. <sup>1</sup>H NMR (CDCl<sub>3</sub>, 400 MHz):  $\delta$  7.87–7.85 (d, 1H, J = 8 Hz), 7.73–7.69 (t, 1H, J = 7.6 Hz), 7.50-7.43 (m, 2H), 3.31 (s, 2H). <sup>13</sup>C{<sup>1</sup>H} NMR (CDCl<sub>3</sub>, 101 MHz):  $\delta$  194.8, 149.2, 137.1, 132.1, 129.0, 126.5, 125.9, 80.3, 39.5. GC-MS (m/z): 158.1  $(M^+ - 2N_2)$ .

HRMS (ESI) m/z: [M + Na]<sup>+</sup> calcd for C<sub>9</sub>H<sub>6</sub>N<sub>6</sub>ONa, 237.04953; found, 237.04953.

*Synthesis of 2,2-Diazido-2,3-dihydroinden-1-one* (1-<sup>15</sup>**N**). Azide 1 was synthesized as described above except that <sup>15</sup>N-labeled sodium azide was used, in which half of the terminal N atoms were labeled. The crude was product-purified via extraction with a cold 19:1 hexane/diethyl ether mixture to yield 1-<sup>15</sup>N as a yellow oil (42.7 mg, 0.198 mmol, 64% yield). IR (neat): 3076, 2927, 2083, 1724, 1608 cm<sup>-1</sup>. <sup>1</sup>H NMR (CDCl<sub>3</sub>, 400 MHz): δ 7.87 (d, 1H, J = 7.7 Hz), 7.71 (td, 1H, J = 7.5, 1.3 Hz), 7.51–7.41 (m, 2H), 3.31 (s, 2H). <sup>13</sup>C{<sup>1</sup>H} NMR (CDCl<sub>3</sub>, 101 MHz): δ 194.8, 149.2, 137.1, 132.1, 129.0, 128.9, 126.6, 126.0, 80.3, 52.4, 39.6. HRMS: calcd for C<sub>9</sub>H<sub>6</sub>O<sup>14</sup>N<sub>4</sub><sup>15</sup>N<sub>2</sub>ONa, 239.04358; found, 239.04360.

Small-Scale Photolysis of 1 in Argon- and Oxygen-Saturated Methanol. Azide 1 (2.0 mg, 0.01 mmol) was dissolved in methanol (10 mL), placed in a test tube that was sealed with a rubber cap, degassed by bubbling with argon or oxygen for 10 min, and irradiated with a Hg arc lamp through a Pyrex filter in 2 h increments. The resulting reaction mixture was analyzed using GC-MS, which revealed some remaining starting material and a complex mixture of photoproducts. The main products were identified as methyl 2-cyanomethylbenzoate (2) and 2-cyanomethylbenzoic acid (3) by injection of authentic samples. After 4 h of irradiation, 2 and 3 were formed in a ratio of 4:1 in argon-saturated methanol, whereas the ratio in oxygen-saturated methanol was 1:1.5.

Preparative-Scale Photolysis of 1 in Argon-Saturated Methanol. A solution of 1 (30 mg, 0.14 mmol) in methanol (30 mL) dried over molecular sieves was irradiated with a mercury arc lamp housed in a Pyrex cooling jacket for 1 h. The solvent was removed under vacuum and dissolved in CDCl<sub>3</sub>. <sup>1</sup>H NMR spectra of the reaction mixture showed the remaining starting material and formation of methyl-2cyanomethylbenzoate (2) and 2-cyanomethylbenzoic acid (3) in the ratio 7:1:0.36, as shown by integration of the signals at 3.31 ppm (1), 3.93 ppm (2), and 4.27 ppm (3). The reaction mixture was redissolved in a minimal amount of methanol (0.10 mL). Some material precipitated (5.6 mg) out of the solution and was confirmed to be polymeric tar by <sup>1</sup>H NMR spectroscopy. The dissolved mixture was separated on a silica column eluted with hexane to yield recovered starting material 1 (5.1 mg, 0.024 mmol, 17% recovery). The column was further eluted with 0.5% ethyl acetate in hexane to yield ester 2 (2 mg, 0.011 mmol, 8% yield). Subsequent washing of the column with methanol yielded (15 mg) polymeric tar.

Synthesis of 2-Cyanomethylbenzoic Acid (3). A solution of methyl 2-cyanomethylbenzoate (AstaTech, commercially available, 0.100 g, 0.57 mmol) in aq NaOH (0.66 mL, 0.66 mmol, 1 M solution) was heated at 40 °C, in a heating mantle controlled with a rheostat, for 1.5 h until no longer transparent. The reaction mixture was cooled to 0 °C and acidified to pH 1 using 6 M aq HCl. The resulting white solid was collected by filtration and characterized as 3 (68.1 mg, 0.423 mmol, 74% yield). The  $^1$ H NMR spectrum of 3 corresponded well with that in the literature.  $^{33}$  mp 112–113 °C (lit.  $^{33}$  mp 114–115 °C).  $^1$ H NMR (CD<sub>3</sub>OD, 400 MHz): δ 8.09 (dd, 1H, J = 7.8, 1.5 Hz), 7.60 (td, 1H, J = 7.5, 1.5 Hz), 7.56–7.53 (m, 1H), 7.47 (td, 1H, J = 7.5, 1.5 Hz), 4.27 (s, 2H). GC–MS (m/z): 161.0 ( $m^+$ ).

# ASSOCIATED CONTENT

#### **Data Availability Statement**

The data underlying this study are available in the published article and its Supporting Information.

#### Supporting Information

The Supporting Information is available free of charge at https://pubs.acs.org/doi/10.1021/acs.joc.4c00499.

IR and NMR spectra of 1-3; UV and IR spectra of irradiated matrices; kinetic traces; and Cartesian coordinates, energies, and vibrational frequencies of 1-5 (PDF)

#### AUTHOR INFORMATION

#### **Corresponding Author**

Anna D. Gudmundsdottir — Department of Chemistry, University of Cincinnati, Cincinnati, Ohio 45221-0172, United States; Ocid.org/0000-0002-5420-4098; Email: anna.gudmundsdottir@uc.edu

#### **Authors**

- Brandi James Department of Chemistry, University of Cincinnati, Cincinnati, Ohio 45221-0172, United States; orcid.org/0000-0002-4425-6783
- H. Dushanee M. Sriyarathne Department of Chemistry, University of Cincinnati, Cincinnati, Ohio 45221-0172, United States
- Upasana Banerjee Department of Chemistry, University of Cincinnati, Cincinnati, Ohio 45221-0172, United States
- Wandana K. S. Henarath Mohottige Department of Chemistry, University of Cincinnati, Cincinnati, Ohio 45221-0172, United States; orcid.org/0009-0002-8016-033X
- Ben Crabtree Department of Chemistry, University of Cincinnati, Cincinnati, Ohio 45221-0172, United States
- Aliz León Department of Chemistry, University of Cincinnati, Cincinnati, Ohio 45221-0172, United States
- Miao Hong Department of Chemistry, University of Cincinnati, Cincinnati, Ohio 45221-0172, United States Javeria Tariq – Department of Chemistry, University of
- Cincinnati, Cincinnati, Ohio 45221-0172, United States Taha Alhayani – Department of Chemistry, University of Cincinnati, Cincinnati, Ohio 45221-0172, United States
- Manabu Abe Department of Chemistry, Graduate School of Advanced Science and Engineering, Hiroshima University, Hiroshima 739-8526, Japan; orcid.org/0000-0002-2013-4394
- Bruce S. Ault Department of Chemistry, University of Cincinnati, Cincinnati, Ohio 45221-0172, United States; orcid.org/0000-0003-3355-1960

Complete contact information is available at: https://pubs.acs.org/10.1021/acs.joc.4c00499

#### **Author Contributions**

<sup>8</sup>H.D.M.S. and U.B. contributed equally.

#### **Author Contributions**

 $^{\perp}$ A.L., M.H., J.T., and T.A. contributed equally.

#### Notes

The authors declare no competing financial interest.

## ACKNOWLEDGMENTS

The authors thank the National Science Foundation (CHE-2102248) and OSC (PES0597) for generous support. H.D.M.S. and U.B. are grateful for Doctoral Enhancement Fellowships from the Department of Chemistry at the University of Cincinnati. A.L. acknowledges an NSF-REU Fellowship (CHE-1950244).

## REFERENCES

- (1) Scaiano, J. C.; Stamplecoskie, K. G.; Hallett-Tapley, G. L. Photochemical Norrish Type I Reaction as a Tool for Metal Nanoparticle Synthesis: Importance of Proton Coupled Electron Transfer. *Chem. Commun.* **2012**, *48*, 4798–4808.
- (2) (a) Encina, M. V.; Lissi, E. A.; Lemp, E.; Zanocco, A.; Scaiano, J. C. Temperature Dependence of the Photochemistry of Aryl Alkyl Ketones. *J. Am. Chem. Soc.* 1983, 105, 1856–1860. (b) Pal, D.; Konar, D.; Sumerlin, B. S. Poly(vinyl ketones): New Directions in

- Photodegradable Polymers. *Macromol. Rapid Commun.* **2023**, 44, 2300126. (c) Lee, K.; Corrigan, N.; Boyer, C. Rapid High-Resolution 3D Printing and Surface Functionalization via Type I Photoinitiated RAFT Polymerization. *Angew. Chem., Int. Ed.* **2021**, 60, 8839–8850.
- (3) (a) Turro, N. J.; Buchachenko, A. L.; Tarasov, V. F. How Spin Stereochemistry Severely Complicates the Formation of a Carbon-Carbon Bond between Two Reactive Radicals in a Supercage. *Acc. Chem. Res.* **1995**, *28*, 69–80. (b) Shiraki, S.; Garcia-Garibay, M. A. Carbon-Carbon Bond Formation by the Photoelimination of Small Molecules in Solution and in Crystals. In *Handbook of Synthetic Photochemistry*; Albini, A., Fagnoni, M., Eds.; Wiley-VCH, 2009; pp 25–66.
- (4) (a) Choi, T.; Peterfy, K.; Khan, S. I.; Garcia-Garibay, M. A. Molecular Control of Solid-State Reactivity and Biradical Formation from Crystalline Ketones. *J. Am. Chem. Soc.* **1996**, *118*, 12477–12478. (b) Peterfy, K.; Garcia-Garibay, M. A. Generation and Reactivity of a Triplet 1,4-Biradical Conformationally Trapped in a Crystalline Cyclopentanone. *J. Am. Chem. Soc.* **1998**, *120*, 4540–4541.
- (5) (a) Mortko, C. J.; Garcia-Garibay, M. A. Green Chemistry Strategies Using Crystal-to-Crystal Photoreactions: Stereoselective Synthesis and Decarbonylation of trans-α,α'-Dialkenoylcyclohexanones. *J. Am. Chem. Soc.* **2005**, 127, 7994–7995. (b) Dotson, J. J.; Perez-Estrada, S.; Garcia-Garibay, M. A. Taming Radical Pairs in Nanocrystalline Ketones: Photochemical Synthesis of Compounds with Vicinal Stereogenic All-Carbon Quaternary Centers. *J. Am. Chem. Soc.* **2018**, 140, 8359–8371.
- (6) Muthukrishnan, S.; Sankaranarayanan, J.; Klima, R. F.; Pace, T. C. S.; Bohne, C.; Gudmundsdottir, A. D. Intramolecular H-Atom Abstraction in  $\gamma$ -Azido-butyrophenones: Formation of 1,5 Ketyl Iminyl Radicals. *Org. Lett.* **2009**, *11*, 2345–2348.
- (7) Sarkar, S. K.; Gatlin, D. M.; Das, A.; Loftin, B.; Krause, J. A.; Abe, M.; Gudmundsdottir, A. D. Laser Flash Photolysis of Nanocrystalline  $\alpha$ -Azido-p-methoxy-acetophenone. *Org. Biomol. Chem.* **2017**, *15*, 7380–7386.
- (8) Singh, P. N. D.; Mandel, S. M.; Robinson, R. M.; Zhu, Z.; Franz, R.; Ault, B. S.; Gudmundsdóttir, A. D. Photolysis of  $\alpha$ -Azidoacetophenones: Direct Detection of Triplet Alkyl Nitrenes in Solution. *J. Org. Chem.* **2003**, *68*, 7951–7960.
- (9) Banerjee, U.; Sarkar, S. K.; Krause, J. A.; Karney, W. L.; Abe, M.; Gudmundsdottir, A. D. Photoinduced  $\alpha$ -Cleavage of 2-Azido-2-phenyl-1,3-indandione at Cryogenic Temperatures. *Org. Lett.* **2020**, 22, 7885–7890.
- (10) Shields, D. J.; Chakraborty, M.; Abdelaziz, N.; Duley, A.; Gudmundsdottir, A. D. Review of Laser Flash Photolysis of Organic Molecules (2015–2018). *Photochemistry* **2019**, *47*, 70–121.
- (11) (a) Neville, A. G.; Brown, C. E.; Rayner, D. M.; Lusztyk, J.; Ingold, K. U. First Direct Detection of Transient Organic Free Radicals in Solution by Time-Resolved Infrared Spectroscopy. Kinetic Studies on Some Acyl Radicals. *J. Am. Chem. Soc.* **1991**, *113*, 1869–1870. (b) Brown, C.; Neville, A.; Rayner, D.; Ingold, K.; Lusztyk, J. Kinetic and Spectroscopic Studies on Acyl Radicals in Solution by Time-Resolved Infrared Spectroscopy. *Aust. J. Chem.* **1995**, *48*, 363–379
- (12) (a) Wasserman, E. Electron Spin Resonance of Nitrenes. In *Progress in Physical Organic Chemistry*; Streitwieser, A., Taft, R. W., Eds.; John Wiley & Sons, Inc., 1971; pp 319–336. (b) Wasserman, E.; Snyder, L. C.; Yager, W. A. ESR of the Triplet States of Randomly Oriented Molecules. *J. Chem. Phys.* **1964**, *41*, 1763–1772.
- (13) Singh, P. N. D.; Mandel, S. M.; Sankaranarayanan, J.; Muthukrishnan, S.; Chang, M.; Robinson, R. M.; Lahti, P. M.; Ault, B. S.; Gudmundsdóttir, A. D. Selective Formation of Triplet Alkyl Nitrenes from Photolysis of  $\beta$ -Azido-Propiophenone and Their Reactivity. *J. Am. Chem. Soc.* **2007**, *129*, 16263–16272.
- (14) Clark, W. D. K.; Steel, C. Photochemistry of 2,3-Diazabicyclo[2.2.2]Oct-2-Ene. J. Am. Chem. Soc. 1971, 93, 6347–6355
- (15) (a) Liu, J.; Mandel, S.; Hadad, C. M.; Platz, M. S. A Comparison of Acetyl- and Methoxycarbonylnitrenes by Computational Methods and a Laser Flash Photolysis Study of Benzoylnitrene.

- J. Org. Chem. 2004, 69, 8583–8593. (b) Kubicki, J.; Zhang, Y.; Wang, J.; Luk, H. L.; Peng, H.-L.; Vyas, S.; Platz, M. S. Direct Observation of Acyl Azide Excited States and Their Decay Processes by Ultrafast Time Resolved Infrared Spectroscopy. J. Am. Chem. Soc. 2009, 131, 4212–4213.
- (16) Pritchina, E. A.; Gritsan, N. P.; Maltsev, A.; Bally, T.; Autrey, T.; Liu, Y.; Wang, Y.; Toscano, J. P. Matrix isolation, time-resolved IR, and computational study of the photochemistry of benzoyl azide. *Phys. Chem. Chem. Phys.* **2003**, *5*, 1010–1018. Dedicated to Professor Dr Z. R. Grabowski and Professor Dr J. Wirz on the occasions of their 75th and 60th birthdays. Electronic supplementary information (ESI) available: Cartesian coordinates and details of the CASSCF/CASPT2 calculations, details of the excited-state calculations on formylnitrene, the full IR spectra, additional results from the TRIR experiments and two tables with results from CASPT2 calculations with different level shifts. See <a href="http://www.rsc.org/suppdata/cp/b2/b209775c/">http://www.rsc.org/suppdata/cp/b2/b209775c/</a>
- (17) Hoyer, H. Die Infrarotabsorption der Isocyanatgruppe. *Chem. Ber.* 1956, 89, 2677–2681.
- (18) Vyas, S.; Kubicki, J.; Luk, H. L.; Zhang, Y.; Gritsan, N. P.; Hadad, C. M.; Platz, M. S. An Ultrafast Time-Resolved Infrared and UV-Vis Spectroscopic and Computational Study of the Photochemistry of Acyl Azides. *J. Phys. Org. Chem.* **2012**, 25, 693–703.
- (19) Desikan, V.; Liu, Y.; Toscano, J. P.; Jenks, W. S. Photochemistry of Sulfilimine-Based Nitrene Precursors: Generation of Both Singlet and Triplet Benzoylnitrene. *J. Org. Chem.* **2007**, *72*, 6848–6859.
- (20) (a) Lee, C.; Yang, W.; Parr, R. G. Development of the Colle-Salvetti Correlation-Energy Formula into a Functional of the Electron Density. Phys. Rev. B: Condens. Matter Mater. Phys. 1988, 37, 785-789. (b) Frisch, M. J.; Trucks, G. W.; Schlegel, H. B.; Scuseria, G. E.; Robb, M. A.; Cheeseman, J. R.; Scalmani, G.; Barone, V.; Petersson, G. A.; Nakatsuji, H.; Li, X.; Caricato, M.; Marenich, A. V.; Bloino, J.; Janesko, B. G.; Gomperts, R.; Mennucci, B.; Hratchian, H. P.; Ortiz, J. V.; Izmaylov, A. F.; Sonnenberg, J. L.; Williams-Young, D.; Ding, F.; Lipparini, F.; Egidi, F.; Goings, J.; Peng, B.; Petrone, A.; Henderson, T.; Ranasinghe, D.; Zakrzewski, V. G.; Gao, J.; Rega, N.; Zheng, G.; Liang, W.; Hada, M.; Ehara, M.; Toyota, K.; Fukuda, R.; Hasegawa, J.; Ishida, M.; Nakajima, T.; Honda, Y.; Kitao, O.; Nakai, H.; Vreven, T.; Throssell, K.; Montgomery, J. A.; Peralta, J. E.; Ogliaro, F.; Bearpark, M. J.; Heyd, J. J.; Brothers, E. N.; Kudin, K. N.; Staroverov, V. N.; Keith, T. A.; Kobayashi, R.; Normand, J.; Raghavachari, K.; Rendell, A. P.; Burant, J. C.; Iyengar, S. S.; Tomasi, J.; Cossi, M.; Millam, J. M.; Klene, M.; Adamo, C.; Cammi, R.; Ochterski, J. W.; Martin, R. L.; Morokuma, K.; Farkas, O.; Foresman, J. B.; Fox, D. J. Gaussian 16. Revision C.01; Gaussian, Inc.: Wallingford, CT, 2016. (c) Chai, J.-D.; Head-Gordon, M. Long-Range Corrected Hybrid Density Functionals with Damped Atom-Atom Dispersion Corrections. Phys. Chem. Chem. Phys. 2008, 10, 6615-6620. (d) Becke, A. D. Density-Functional Thermochemistry. III. The Role of Exact Exchange. J. Chem. Phys. 1993, 98, 5648-5652.
- (21) (a) Noodleman, L.; Baerends, E. J. Electronic Structure, Magnetic Properties, Esr, and Optical Spectra for 2-Iron Ferredoxin Models by Lcao-X.Alpha. Valence Bond Theory. J. Am. Chem. Soc. 1984, 106, 2316–2327. (b) Yamaguchi, K.; Jensen, F.; Dorigo, A.; Houk, K. N. A spin correction procedure for unrestricted Hartree-Fock and Møller-Plesset wavefunctions for singlet diradicals and polyradicals. Chem. Phys. Lett. 1988, 149, 537–542.
- (22) Feng, R.; Lu, Y.; Deng, G.; Xu, J.; Wu, Z.; Li, H.; Liu, Q.; Kadowaki, N.; Abe, M.; Zeng, X. Magnetically Bistable Nitrenes: Matrix Isolation of Furoylnitrenes in Both Singlet and Triplet States and Triplet 3-Furylnitrene. J. Am. Chem. Soc. 2018, 140, 10–13.
- (23) Ault, B. S. Infrared Spectra of Argon Matrix-Isolated Alkali Halide Salt/Water Complexes. J. Am. Chem. Soc. 1978, 100, 2426–2433.
- (24) Sarkar, S. K.; Upul Ranaweera, R. A. A.; Merugu, R.; Abdelaziz, N. M.; Robinson, J.; Day, H. A.; Krause, J. A.; Gudmundsdottir, A. D. Comparison of the Photochemistry of Acyclic and Cyclic 4-(4-Methoxy-Phenyl)-4-Oxo-but-2-Enoate Ester Derivatives. *J. Phys. Chem. A* **2020**, *124*, 7346–7354.

- (25) Banerjee, U.; Karney, W. L.; Ault, B. S.; Gudmundsdottir, A. D. Photolysis of 5-Azido-3-phenylisoxazole at Cryogenic Temperature: Formation and Direct Detection of a Nitrosoalkene. *Molecules* **2020**, 25, 543.
- (26) Ranaweera, R. A. A. U.; Scott, T.; Li, Q.; Rajam, S.; Duncan, A.; Li, R.; Evans, A.; Bohne, C.; Toscano, J. P.; Ault, B. S.; Gudmundsdottir, A. D. Trans—Cis Isomerization of Vinylketones through Triplet 1,2-Biradicals. *J. Phys. Chem. A* **2014**, *118*, 10433—10447.
- (27) (a) Bauernschmitt, R.; Ahlrichs, R. Treatment of Electronic Excitations within the Adiabatic Approximation of Time Dependent Density Functional Theory. *Chem. Phys. Lett.* **1996**, *256*, 454–464. (b) Stratmann, R. E.; Scuseria, G. E.; Frisch, M. J. An Efficient Implementation of Time-Dependent Density-Functional Theory for the Calculation of Excitation Energies of Large Molecules. *J. Chem. Phys.* **1998**, *109*, 8218–8224.
- (28) Halls, M. D.; Velkovski, J.; Schlegel, H. B. Harmonic frequency scaling factors for Hartree-Fock, S-VWN, B-LYP, B3-LYP, B3-PW91 and MP2 with the Sadlej pVTZ electric property basis set. *Theor. Chem. Acc.* **2001**, *105*, 413–421.
- (29) Gonzalez, C.; Schlegel, H. B. Reaction Path Following in Mass-Weighted Internal Coordinates. *J. Phys. Chem. Phys.* **1990**, 94, 5523–5527.
- (30) Boger, D. L.; Zhu, Y. Diels-Alder Reactions of Cyclopropenone Ketals: A Concise Tropolone Annulation Applicable to Rubrolone C Ring Introduction. *J. Org. Chem.* **1994**, *59*, 3453–3458.
- (31) House, H. O.; McDaniel, W. C. Perhydroindan Derivatives. 18. The Use of Indenone Ketals as Dienophiles. *J. Org. Chem.* 1977, 42, 2155–2160.
- (32) Kösel, T.; Drager, G.; Kirschning, A. Oxidative Azidations of Phenols and Ketones Using Iodine Azide after Release from an Ion Exchange Resin. *Org. Biomol. Chem.* **2021**, *19*, 2907–2911.
- (33) Gretler, R.; Askitol, E.; Kühne, H.; Hesse, M. Die Massenspektrometrische retro-Diels-Alder-Reaktion: 1,2,3,4-Tetrahydroisochinolin und 1,2,3,4-Tetrahydronaphthalin (Tetralin). 31. Mitteilung über Massenspektrometrische Untersuchungen. *Helv. Chim. Acta* 1978, 61, 1730–1755.